Exploratory study of Polycyclic Aromatic Hydrocarbons occurrence and distribution in manure pyrolysis products

I. Adánez-Rubio[1*], P. de Blas[1], F. Viteri[1,2], I. Fonts[1,3], G. Gea[1], M.U. Alzueta[1]

[1]*Aragón Institute of Engineering Research (I3A), Department of Chemical and Environmental Engineering, University of Zaragoza, Zaragoza 50018, Spain*

[2]*Universidad UTE, Facultad de Ciencias de la Ingeniería e Industrias, Quito, Ecuador*

[3]*Área de Química y Medio Ambiente, Centro Universitario de la Defensa (CUD) de Zaragoza- Academia General Militar, 50090, Zaragoza, Spain*

*Corresponding author: Phone: +34976733977, e-mail address: iadanez@icb.csic.es

Abstract

The occurrence and distribution of polycyclic aromatic hydrocarbons (PAH) have been investigated in the products derived from the pyrolysis of pig manure at low temperatures (<550 ºC) in a fixed bed reactor. The focus was on the sixteen PAH identified as priority pollutants by the US Environment Protection Agency (EPA). The pyrolysis does not generate a significant additional amount of EPA-PAH to that existing in the original pig manure, under the operational conditions studied (<550 ºC). While the total EPA-PAH yield does not indicate a notable dependence on the pyrolysis temperature, the EPA-PAH distribution among the three pig manure pyrolysis products as well as the speciation changed significantly with the temperature. The proportion of heavy PAH species increased as the temperature increased. The initial EPA-PAH in the manure samples plays a significant role in both their concentration and speciation in the biochar. The relationship of the EPA-PAH concentration and speciation in the biochar with those of the raw material was corroborated with a cow manure sample and the biochars obtained from its pyrolysis. For this reason, feedstocks with low EPA-PAH concentrations are recommended in order to obtain biochars with concentrations below the maximum allowed threshold established for their use as a soil enhancer by the International Biochar Initiative (IBI) and in the European Biochar Certificate.

Keywords: pig manure, co-digested cow manure, pyrolysis, polycyclic aromatic hydrocarbon (PAH), biochar.

1. Introduction

The conversion of biomass to biochar has long been recognized as a favorable valorization strategy. Biochar addition to soils increases crop yields [1] and the organic carbon in the biochar remains fixed for many years, which prevents its mineralization and potential release as CO_2 [2, 3]. Utilization of waste biomass, such as sewage sludge, municipal solid waste or livestock manure, is not only considered an ecofriendly practice, but can also pave the way to an effective valorization of these waste streams [4]. Converting livestock manure to biochar, instead of using it directly as organic amendment, could therefore result in a more favorable CO_2 balance [3].

However, biochar usually contains toxic polycyclic aromatic hydrocarbons (PAH) which could end up in the soil and consequently might find their way into water reservoirs and even into the food chain. This problem has long been recognized. As a result, threshold values for the 16 high priority PAH (see Fig. 1) identified by the US Environmental Protection Agency have been proposed by associations promoting biochar usage, such as the International Biochar Initiative (IBI) and the European Biochar Certificate Foundation (EBC), to ensure the safe application of biochar [5, 6]. IBI established a threshold value for the total sum of the 16 EPA-PAH (Σ16 EPA-PAH) of 6 mg·kg^{-1} for Europe and 300 mg·kg^{-1} for Australia, while EBC requires the Σ16 EPA-PAH to be below 12 mg·kg^{-1} for basic grade biochar and below 4 mg·kg^{-1} for premium grade biochar [5, 6].

Σ16 EPA-PAH levels in biomass and waste biomass-derived biochars reported in the literature show significant variability, with values ranging from 0.07 mg·kg^{-1} to 3000 mg·kg^{-1} [7-13]. The operating conditions, particularly the temperature, the feedstock, and the type of reactor have been reported to play a significant role in the Σ16 EPA-PAH levels in biochar, although previous works have presented some contradictory results regarding the effect of these factors. The pyrolysis temperature has an enormous effect on the biochar properties [14, 15] and therefore the understanding of its effect on the PAH content in biochar is another factor that could help to select the appropriate temperature. Freddo et al. [12] (300 – 600 ℃) found that the Σ16 EPA-PAH concentration in the biochar samples obtained from four different biomass materials (redwood, bamboo, maize and rice) decreases as the temperature increases. Hale et al. [10], who analyzed 50 biochar samples obtained in a wide temperature range (250-900 ℃), also found that the Σ16EPA-PAH concentration generally decreases as the temperature increases. However, Kloss et al. [11] (400-525 ℃) obtained a different

temperature effect on the Σ16 EPA-PAH concentration for each of the three raw materials studied (straw, poplar wood and spruce wood). Keiluweit et al. [16] (100-700 ºC), Zielińska and Oleszczuk [17] (500-700 ºC) and Buss et al. [9] (350-750 ºC) found different effects of the influence of temperature on the Σ16 EPA-PAH concentration, including the maximum or minimum values within the intervals of temperature studied, and decreasing or increasing trends.

Buss et al. [9] explained the discrepancies in the impact of temperature by its positive effect in both the formation of PAH and their volatilization from biochar during pyrolysis, both processes being favored by an increase in the temperature, but presenting a contrary effect on the final PAH concentration in biochar. It seems that at a high pyrolysis temperature (over 750 ºC) [8, 9] or under gasification conditions (750-850 ºC) [7, 10], the formation of PAH is so significant that the biochar obtained at these operating conditions presents the highest Σ16 EPA-PAH concentration independently of the raw material or the technology used. However, many years of research in this topic did not yield a clear understanding of how to control the PAH content in biochars obtained at typical pyrolysis temperatures for biochar production (<650 ºC), probably because at these temperatures the formation of PAH is not so significant and the effect of volatilization is more noticeable. The important effect of volatilization in PAH levels in biochar was corroborated by the study of the effect of the carrier gas flow-rate conducted by Buss et al. [9]. These authors found that increasing the carrier gas flow-rate (0.0-6.7 L·min^{-1}) through the bed during biomass pyrolysis in a fixed bed reactor decreased the Σ16 EPA-PAH level in biochars because of the enhanced devolatilization. Apart from the operating conditions, another important factor affecting the PAH concentration in biochar is the raw material. However, existing studies have not been able to establish correlations between the content of macro-components in biomass (lignin, cellulose and hemicellulose) and the PAH level in biochar. For example, some studies have pointed out that lignin-rich feedstocks yield high Σ16 EPA-PAH [18, 19], while in others this was not observed [9, 20]. Recent studies conducted at temperatures lower than 700 ºC, in which the PAH levels in the raw materials and in the biochars have been compared, have shown that the Σ16 EPA-PAH concentration in both solid matrices are of the same order of magnitude [21] or significantly lower in the biochars than in the feedstock [17]. These results suggest that, at low temperatures (<650 ºC), the formation of PAH is not significant and the final concentration of PAH in biochar would be determined by the amount of PAH contained in the feedstock and by the

extent of the volatilization from the solid matrix during the pyrolysis reaction. Therefore, in order to control the PAH concentration in the biochar obtained at low temperatures (<650 ºC), it would be necessary to know the contribution of each process (formation and volatilization) to the final PAH concentration for different feedstocks, technologies and operating conditions. A good strategy to know the contribution of these processes to the final Σ16 EPA-PAH content in biochar could be to evaluate both the content of EPA-PAH in the feedstock and the distribution of the EPA-PAH among the three pyrolysis products (biochar, liquid and gas). However, in the few studies existing in the literature in which the distribution of EPA-PAH among pyrolysis products has been studied, the initial content of PAH in the raw materials was not determined [22, 23].

It is important to clarify the possible relation between the content of PAH in the raw materials and in the biochars. This is particularly important for waste-derived types of biomass, such as livestock manures, which due to their origin or pretreatment are more likely to contain substantial amounts of PAH [24-26]. This raises the question of how to manage PAH-containing biomass such as livestock manure. Its direct application as an organic amendment in agriculture could release the adsorbed PAH into the soil and therefore cause the same problems as those discussed above for biochar. If the conversion of livestock manure to biochar under controlling conditions reduced the Σ16 EPA-PAH level, then such a procedure would be beneficial. In the present experimental study, the following questions are addressed: What is the relationship, if any, between the Σ16 EPA-PAH concentration in the raw materials and in biochars? Will the total amount of PAH change after pyrolysis, i.e. is there significant PAH net formation? Will pyrolytic conversion form, destroy, transform or just volatilize the PAH contained in manure to biochar? How will the PAH be distributed among the three pyrolysis products? Will the PAH composition in the original manure change during pyrolysis? Will the biochar toxicity change due to the pyrolysis treatment?

In order to answer these questions, the Σ16 EPA-PAH inventory before and after the reaction and their individual distribution among the three pyrolysis products (gas, solid and liquid) during manure pyrolysis at low temperatures (350 – 550 ºC) has been studied with a sample of pig manure stored outdoors. In order to study the possible relation between the PAH in the pig manure sample and in its derived biochars, the Σ16 EPA-PAH levels and the toxicity of the biochars obtained at the different pyrolysis temperatures have been compared with those of the feedstock using two different

manures, pig manure and co-digested cow manure. The Σ16 EPA-PAH level in the co-digested cow manure is two orders of magnitude lower than that in the pig manure, which will help to identify the influence of the feedstock EPA-PAH levels in those of the biochars obtained.
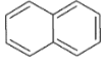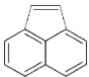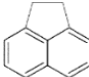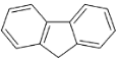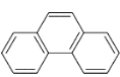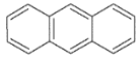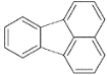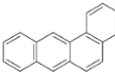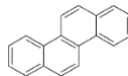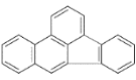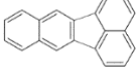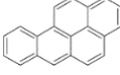
16 priority EPA-PAH					
2 rings	3 rings				
Naphthalene Abbr: NAPH M: 128 g/mol BP: 218 ºC [27]	Acenaphthylene Abbr: ACNY M:152 g/mol BP: 280 ºC [27]	Acenaphthene Abbr: ACN M: 154 g/mol BP: 279 ºC [27]	Fluorene Abbr: FLUO M: 166 g/mol BP: 295 ºC [27]	Phenanthrene Abbr: PHEN M: 178 g/mol BP: 340 ºC [27]	Anthracene Abbr: ANTH M: 178 g/mol BP: 340 ºC [27]
4 rings					
Fluoranthene Abbr: FANTH M: 202 g/mol BP: 384 ºC [27]		Pyrene Abbr: PYR M: 202 g/mol BP: 404 ºC [27]	Benzo[a]anthracene Abbr: B[a]A M: 228 g/mol BP: 438 ºC [27]		Chrysene Abbr: CHR M: 228 g/mol BP: 448 ºC [27]
5 rings				6 rings	
Benzo[b]fluo-ranthene Abbr: B[b]F M: 252 g/mol BP: 481 ºC [28]	Benzo[k]fluo-ranthene Abbr: B[k]F M: 252 g/mol BP: 480 ºC [27]	Benzo[a]pyrene Abbr: B[a]P M: 252 g/mol BP: 496 ºC [28]	Dibenz[a,h]an-thracene Abbr: DB[ah]A M: 278 g/mol BP: 797 ºC [29]	Indeno[1,2,3-cd]pyrene Abbr:I[123-cd]P M: 276 g/mol BP: 536 ºC [30]	Benzo[g,h,i]pe-rylene Abbr: B[ghi]P M: 276 g/mol BP: 550 ºC [28]

Fig. 1. 16 EPA-PAH studied in the present work. BP: Boiling Point.

2. Experimental section

2.1 Materials

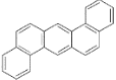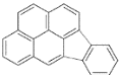The study of the EPA-PAH production and distribution has been conducted with outdoor-stored pig manure (OS-PM), which was not subjected to any stabilization treatment apart from its outdoor storage (O0°12'39.53", N40°56'14.03") at ambient conditions during several months. Apart from the OS-PM, co-digested cow manure (CD-CM) was also used for the biochar study. The CD-CM was supplied by the HTN Biogas Company located in Caparroso (Navarra, Spain) and was obtained by anaerobic co-digestion of cattle manure with agro-industrial wastes. The anaerobically co-digested

manure was separated in a decanter centrifuge and prepared for the experiment by drying at 105 ºC. The main characteristics of both residues are shown in Table 1. The particle size of both was between 0.075 to 5 mm.

Table 1. Ultimate, proximate and metal composition of CD-CM and OS-PM as received.

	OS-PM	CD-CM		OS-PM	CD-CM
C (wt.%)[a]	27.3	31.7	Al (mg g^{-1})[f]	13.9	8.1
H (wt.%)[a,b]	5.3	4.2	Ca (mg g^{-1})[f]	170.9	49.5
N (wt.%)[a]	2.0	1.9	Fe (mg g^{-1})[f]	23.9	7.0
O (wt.%)[a,b,c]	32	50.7	K (mg g^{-1})[f]	49.9	7.7
S (wt.%)[a]	1.0	0.5	Mg (mg g^{-1})[f]	41.1	7.2
Ash (wt.%)[d]	32.7	20	Na (mg g^{-1})[f]	14.5	4.3
Moisture (wt.%)[e]	20.2 ± 0.4	13	P (mg g^{-1})[f]	45.8	13.5

[a] *Ultimate analysis was performed using a Leco TruSpec® Micro Elemental Analyzer.*
[b] *The percentages of H and O include contribution from moisture.*
[c] *O was calculated by difference as O(wt.%) = 100-C(wt.%)-H(wt.%)-N(wt.%)-S(wt.%)-ash(wt.%).*
[d] *According to ISO-18122-2015.*
[e] *According to ISO-589-1981.*
[f] Metal concentration determined by inductively coupled plasma optical emission spectrometry (ICP-OES).

The EPA-PAH concentration in both materials was analyzed following the same method as that utilized with the biochar samples obtained in the experiments (see Section 2.3). The results obtained from these analyses are shown in Table 4 (see Section 3.3). According to these analyses, the total EPA-PAH concentration in CD-CM (0.85 mg·kg^{-1}) is twice the order of magnitude lower than the concentration in OS-PM (115 mg·kg^{-1}). This difference is especially interesting for checking the relationship between the EPA-PAH occurrence in feedstocks and their biochars.

The concentration of total EPA-PAH determined in CD-CM is in the same range as those reported for raw cow manure samples by Zhao et al. [25] (0.237-0.542 mg·kg^{-1}), and Qiu et al. [21] (0.562 mg·kg^{-1}), lower than those reported for co-digested cow manure by Suominen et al. [26] (mean of 6 solid digestate samples 5.20 mg·kg^{-1}) and significantly higher than those also determined in cow manures by Rey-Salgueiro et al. [24] (9·10^{-3} mg·kg^{-1}). The high concentration of total PAH in OS-PM in comparison with the other manure samples might be due to the air deposition of PAH during its outdoor storage in lagoons (O0°12'39.53", N40°56'14.03"). Deposition rates of PAH reported in the literature such as 70–670 ng·m^{-2}·d^{-1} [31] or 18.8–278 ng·m^{-2}·d^{-1} [32] and its storage during months in the lagoons could justify the high concentrations determined in OS-PM.

OS-PM only showed the presence of PHEN, FANTH and PYR, which were also some of the most abundant PAH species in CD-CM (see Table 4). Apart from these three PAH species, NAPH, B[a]P and B[ghi]P were also present in high concentrations in CD-CM (see Table 4). The speciation found, with PHEN being outstanding as very abundant, is consistent with that reported in the literature for these types of materials [25, 26].

2.2 Experimental set-up

The pyrolysis experiments were performed in a fixed bed reactor shown schematically in Fig. 2. The experimental system consists of two different zones: the reaction zone and the condensation zone. The fixed bed reactor (5), a vertical cylinder of stainless steel 316-L, was heated by an electrical furnace. In the experiments, 300 g of pig manure were loaded inside the reactor, which corresponds to ¾ of the reactor volume. A flow rate of 0.25 $dm^3 \cdot min^{-1}$ (STP) N_2, as inert gas, was fed into the lower zone of the reactor bed. The vapors passed through an externally heated hot filter (8) to retain char fines elutriated from the reactor. The hot filter and first condenser were joined by a 10 cm stainless steel tube. The hot filter was kept at the same temperature as the temperature of the pyrolysis reactor. The connecting tube was isolated with glass wool in order to maintain the hot filter temperature and to avoid the condensation of tar compounds.
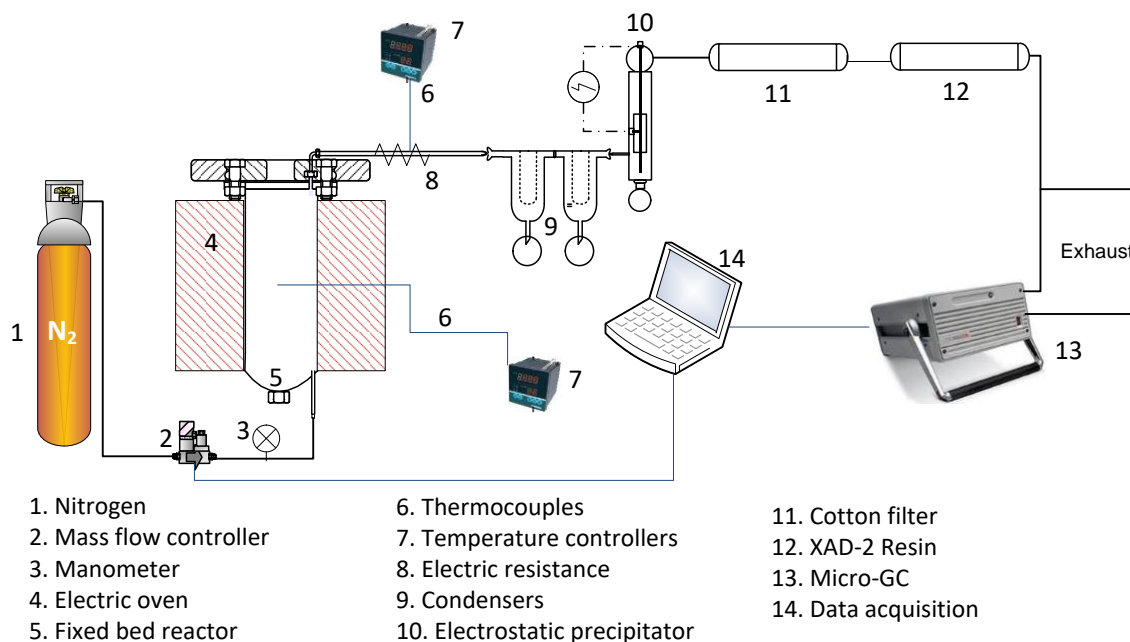
Fig. 2. Schematic view of the fixed bed reactor set-up.

1. Nitrogen
2. Mass flow controller
3. Manometer
4. Electric oven
5. Fixed bed reactor

6. Thermocouples
7. Temperature controllers
8. Electric resistance
9. Condensers
10. Electrostatic precipitator

11. Cotton filter
12. XAD-2 Resin
13. Micro-GC
14. Data acquisition

The condensation zone consisted of two condensers refrigerated by a chiller at 0 ℃ (9) and an electrostatic precipitator (10). In this zone, the condensable vapors (both organic compounds and water) were collected, and a known amount of methanol was used as washing liquid for these three devices and the stainless steel tube connecting the hot filter and the first condenser. A cotton filter (11) was placed downstream of the condensation zone. Char and liquid yields were calculated by weight difference of the devices used for their collection before and after the experiment. Following the procedure described by Sánchez et al. [33], the PAH present in the outlet gas were collected in a thin tube of 300 mm in length and 10 mm of external diameter packaged with XAD-2 resin (12). The resin was divided in two parts: (a) the first part containing 3 g of resin was used to collect the PAH and (b) the second part, consisting of 2 g of resin, was used as a blank. Both parts were separated by quartz wool. Finally, the composition (vol.%) of the non-condensable gases was analyzed continuously by a micro gas chromatograph (Agilent MicroGC 3000A) connected online (13), which took a gas sample every 3 minutes during the experiment. The gas species analyzed were CO_2, CO, CH_4, C_2H_6, C_2H_2, H_2S, H_2 and N_2. Nitrogen served as an internal standard for the calculation of the mass flow of each gas species. For the determination of the total mass

of each gas species, an integration of their mass flows with the experimental time was performed.

The pyrolysis experiments were carried out at three different final temperatures: 350, 450 and 550 ºC using a heating rate of 8 ºC·min^{-1}. Once the final pyrolysis temperature was reached, it was maintained for 30 min. The experiments were replicated to evaluate the repeatability of the results. The biochars were named CD-CM-X and OS-PM-X, with X indicating the final pyrolysis temperature (350, 450 and 550 ºC). For example, OS-PM-350 stands for biochar produced from outdoor-stored pig manure at 350 ºC. The feedstocks were referred to as OS-PM and CD-CM.

2.3 PAH analysis

The analyses of the EPA-PAH concentration in the solid product and the resin used to collect the EPA-PAH from the gas product were carried out following the methodology proposed by Sánchez et al. [33], which is based on the recommendations of the 8270D EPA method. This methodology has been successfully applied in a number of earlier studies addressing the quantification of EPA–PAH from the pyrolysis of different hydrocarbons over a wide range of operating conditions, (e. g.[33-36]). It consists of two steps: a solid-liquid Soxhlet extraction with dichloromethane (DCM), followed by concentration, and the subsequent analysis of the extracted EPA-PAH by gas GC-MS.

In the extraction method, the sample (manure, biochar and XAD-2 resin) was submitted to a Soxhlet extraction during 24 h using a total amount of 200 mL of DCM and 4 extraction cycles per hour [33]. A mixture of five deuterated PAH (Mix 26, Dr. Ehrenstorfer-Schäfers acenaphthene-d10, chrysene-d12, naphthalene-d8, perylene-d12 and phenanthrene-d10) was used as an internal standard to correct for possible losses of analytes during sample handling and extraction. The sample extracts were reduced to approximately 5 mL by rota-evaporation (bath temperature around 308 K). They then underwent micro-concentration using a gentle nitrogen stream to give a final volume of 1.5 mL [33]. In the case of the liquid product, a known volume of the mixture of the internal standards was added to a known volume of liquid sample (liquid product and washing solvent) and placed in the chromatographic vial.

The EPA-PAH were identified and quantified by GC-MS. The GC-MS system (Agilent 7890A gas chromatograph coupled to an Agilent 5975C mass selective detector) was operated in Selected Ion Monitoring (SIM) mode. A medium-polarity capillary column, DB-17Ms (Agilent 60 m x 0.25 mm x 0.25 µm), was used. An EPA-PAH standard mixture (PAH-Mix 63, Dr. Ehrenstorfer-Schäfers) containing the 16 EPA-PAH was employed for calibration purposes following the internal standard method. Calibration curves with eight concentration levels were constructed. The slope, intercept and regression of the linear calibration curves are provided in Table S1 of the Supplementary Material. The limits of detection (LOD) and quantification (LOQ) were established with 95% confidence [33]. This method allows quantification of the different EPA-PAH with a high degree of sensitivity because it operates in SIM mode, selecting specific ions for the 9 defined time windows. This chromatographic method was also utilized for the determination of the EPA-PAH concentration in the pyrolysis liquid product collected from the condensers with a known amount of methanol.

Grouped standard deviations, calculated as the square root of the mean square for error in the analysis of variance (ANOVA) [37], were used as an estimation of the sampling variability. These values are shown as error bars in the figures.

The concentration of the EPA-PAH determined in the feedstocks and in the biochars obtained from the pyrolysis was used to assess their toxicity. The toxicity of each EPA-PAH relative to B[a]P was determined by using the toxicity equivalent factor (TEF), which is a parameter used to express the toxicity of each EPA-PAH relative to B[a]P(reference compound) [38]. Table S2 shows the TEF values for each EPA-PAH analyzed in the present work. The toxicity of a sample expressed as benzo[a]pyrene equivalent concentration (B[a]P-eq) can be calculated using the TEF values as follows:

$$B[a]P - eq = \sum_{i=1}^{n}(TEF_i) \cdot [PAH_i] \qquad\qquad \text{(Eq. 1)}$$

where $[PAH_i]$ means PAH concentration in the solid sample.

3. Results and discussion

The experimental results for the distribution of the pyrolysis products obtained from both feedstocks are shown in Table 2. These results have been used to determine the EPA-PAH yields. The trends observed for the product distribution with the temperature agree with those obtained in previous works on pyrolysis with similar feedstocks [39, 40].

Table 2. Product yields (wt.%) and mass balance (%) expressed as average +/- grouped standard deviation obtained in the different pyrolysis experiments.

Reactor	OS-PM			CD-CM		
Temperature (ºC)	350	450	550	350	450	550
Solid (wt. %)	49 ± 2	43 ± 2	43 ± 2	51 ± 2	47 ± 2	45 ± 2
Liquid (wt. %)	43 ± 1	46 ± 1	42 ± 1	37 ± 1	37 ± 1	38 ± 1
Gas (wt. %)	5 ± 1	7 ± 1	8 ± 1	8 ± 1	14 ± 1	16 ± 1
Balance (%)	98 ± 4	96 ± 4	93 ± 4	96 ± 4	98 ± 4	99 ± 4

3.1 Occurrence of total EPA-PAH in pig manure pyrolysis

Table 3 shows the concentration of the $\Sigma 16$ EPA-PAH in the OS-PM feedstock, and the total $\Sigma 16$ EPA-PAH yield and closure of the mass balances obtained from the pyrolysis experiments at the three different temperatures (350, 450 and 550 ºC).

Table 3 Concentration of the $\Sigma 16$ EPA-PAH in the OS-PM feedstock, and total $\Sigma 16$ EPA-PAH yield expressed as average +/- grouped standard deviation and closure of the $\Sigma 16$ EPA-PAH mass balances obtained from the pyrolysis experiments.

	OS-PM	OS-PM-350	OS-PM-450	OS-PM-550
$\Sigma 16$ EPA-PAH total yield (mg·kg^{-1} of OS-PM)	115	118 ± 9	122 ± 9	108 ± 9
$\Sigma 16$ EPA-PAH mass balance (%)		103	106	94

The amounts of EPA-PAH detected in the pyrolysis products of OS-PM at the three temperatures investigated are very similar to the amount of PAHs found in the raw OS-PM. Taking into account the experimental error, neither significant formation nor

significant consumption of Σ16 EPA-PAH is observed at any of the pyrolysis temperatures used in the OS-PM experiments.

3.2 Effect of the pyrolysis temperature on the EPA-PAH distribution and speciation

The distribution of Σ16 EPA-PAH in the three pyrolysis products obtained from OS-PM is presented in Fig. 3. It can be observed that the EPA-PAH yields in the gas fractions are almost negligible. Even the highest yields obtained at 550 ℃ are at least two orders of magnitude lower than those found in the char or liquid products. This means that EPA-PAH either stay in the solid fraction or they are efficiently condensed in the current setup.

In general, the Σ16 EPA-PAH yields in the liquid and char are of similar magnitude, with the exception of the experiment performed at 450 ℃, in which the yield of Σ16 EPA-PAH in the liquid was approximately double that in the biochar.

The increase in the Σ16 EPA-PAH yield in the liquid product from 350 ℃ to 450 ℃ can be explained by an increased evaporation and entrainment of these compounds from the solid matrix. A further increase to 550 ℃ favors growth of volatile PAH from other less volatile ones (bigger ones), which would remain adsorbed in the solid matrix due to their higher boiling point. The EPA-PAH yields in biochar obtained in this work suggest that a large fraction of the EPA-PAH molecules in pig manure are strongly adsorbed to the solid, preventing them from being flushed away by the gas stream within the temperature range studied. These results clearly deviate from the work by Fagernäs et al. [22] who observed that PAH formed in the pyrolysis of birch at 450 ℃ in a batch retort ended up almost exclusively in the liquid and gas products, while only 0.6% remained in the solid. The experiments by Fagernäs et al. [22] were performed at very low heating rates and much longer solid residence times than those used in the present work. Another important difference is the feed material: lignocellulosic biomass [22] as opposed to the PAH contaminated pig manure used in this study.
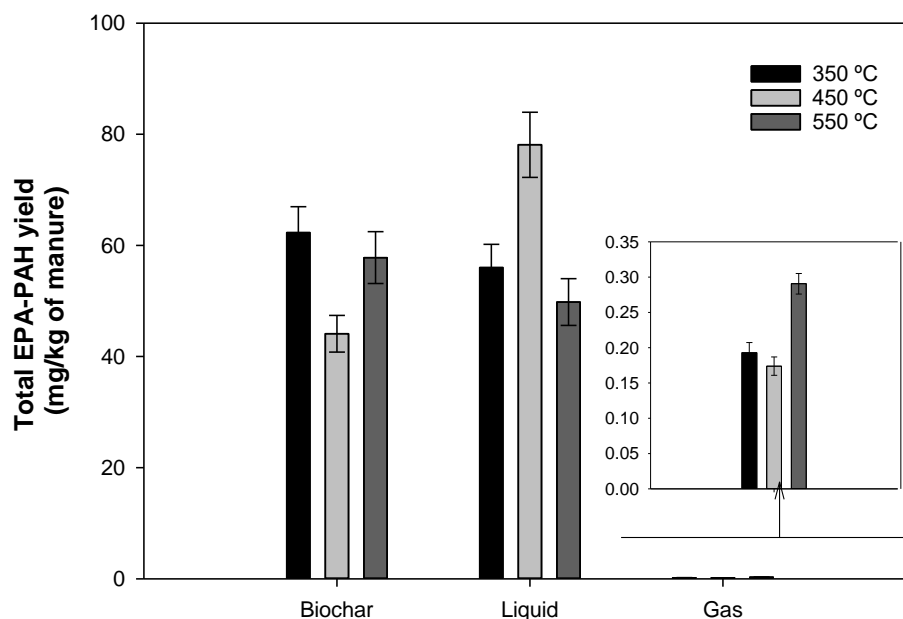
Fig. 3. Σ16 EPA-PAH yield obtained in the three pyrolysis products from OS-PM (error bars show grouped standard deviation).

Fig. 4 shows the individual EPA-PAH yields obtained in the OS-PM pyrolysis experiments carried out at the different pyrolysis temperatures (350, 450 and 550 ℃). At the temperatures studied, new EPA-PAH species, apart from the three identified in the feedstock (PHEN, FANTH and PYR), have been detected. The EPA-PAH compounds with relatively high yields are NAPH, FLUO, PHEN, FANTH and (B[ghi]P). Except for B[ghi]P, the majority compounds have low or medium molecular weights. This can be attributed to the relatively low temperatures utilized in the pyrolysis experiments [41]. DB[ah]A was the only EPA-PAH not detected in the pyrolysis products obtained from OS-PM at any of the temperatures studied.

The results of this current study show that temperature affects the speciation of EPA-PAH. EPA-PAH of low molecular weight with two to four aromatic rings dominate at the temperatures of 350 and 450 ℃; NAPH, ACNY, FLUO, PHEN and FANTH are found to be particularly abundant. At these temperatures (350 and 450 ℃), some high molecular weight EPA-PAH such as I[123-cd]P and B[ghi]P are also present. At 550 ℃, but also at 450 ℃, the formation of EPA-PAH with four or more aromatic rings becomes more significant, indicating that at this temperature the formation of high molecular weight EPA-PAH is favored. At this temperature (550 ℃), the yields of the compounds CHR, B[a]A, B[b]F, B[k]F, and B[a]P increased. These results indicate that

EPA-PAH are reactive at low pyrolysis temperatures and that the increased importance of higher molecular weight PAH at higher temperatures may be due to the fusion of smaller PAH to larger ones, leading to the decline of the H/C ratio. The increase in the presence of higher molecular weight PAH with the temperature was also observed by other authors addressing the pyrolysis of sewage sludge, another biological residue, within a similar interval of temperatures [41, 42].

The mechanism that forms larger EPA-PAH molecules under the present experimental conditions is not clear. Radical reactions, typically observed at high temperatures in the gas phase, are presumably of little importance at the low temperatures used in the present study. One possibility could be that the ash content may act as catalyst for EPA-PAH fusion, enhancing the recombination of smaller PAH molecules and their condensation into larger more stable ones [43]. However, mechanistic studies would be needed to support such speculation. Moreover, although the gas-phase HACA (Hydrogen-Abstraction/Carbon-Addition) mechanism is initiated at significantly higher temperatures (around 800 ºC), the high ash content could promote the formation of precursors of the HACA mechanism, which could also help the low molecular weight PAH to grow through the HACA route [44].

In summary, considering the different EPA-PAH species obtained in the pyrolysis products and the closure of the EPA-PAH mass balance of the experiments carried out at the three temperatures studied (see Table 3), it seems that the EPA-PAH species originally present in the feedstock are transformed into other EPA-PAH species during pyrolysis.
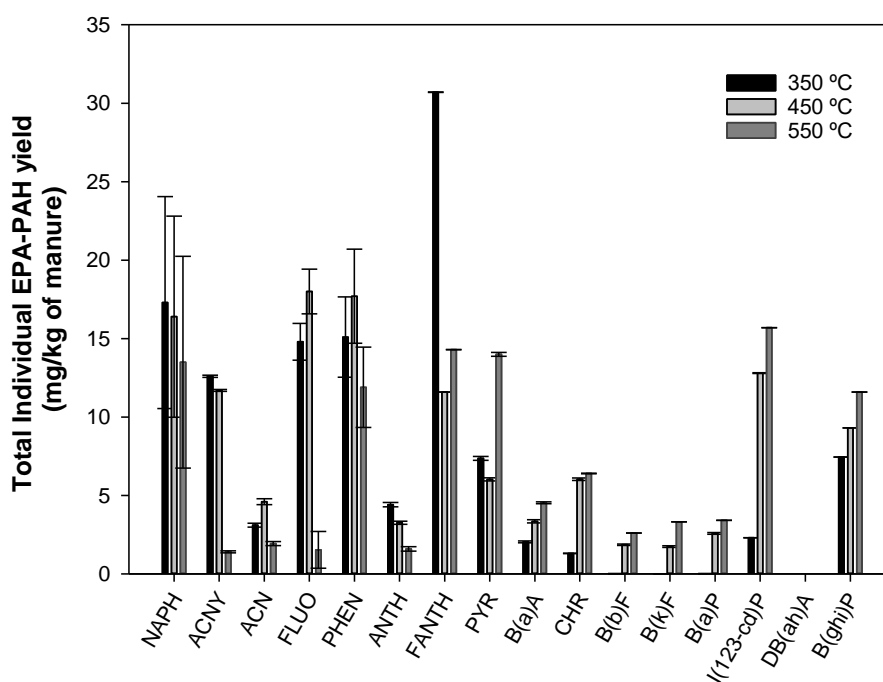
Fig. 4. Individual EPA-PAH yields obtained in each OS-PM pyrolysis experiment (error bars show grouped standard deviation).

The individual EPA-PAH yields obtained at the different pyrolysis temperatures in each of the products are shown in Fig. 5a (gas), Fig. 5b (liquid) and Fig. 5c (biochar). Some of the GC-MS chromatographs for the EPA-PAH analysis in gas, liquid and biochar obtained at 450 ℃ from OS-PM are also shown as an example in Fig. S1.
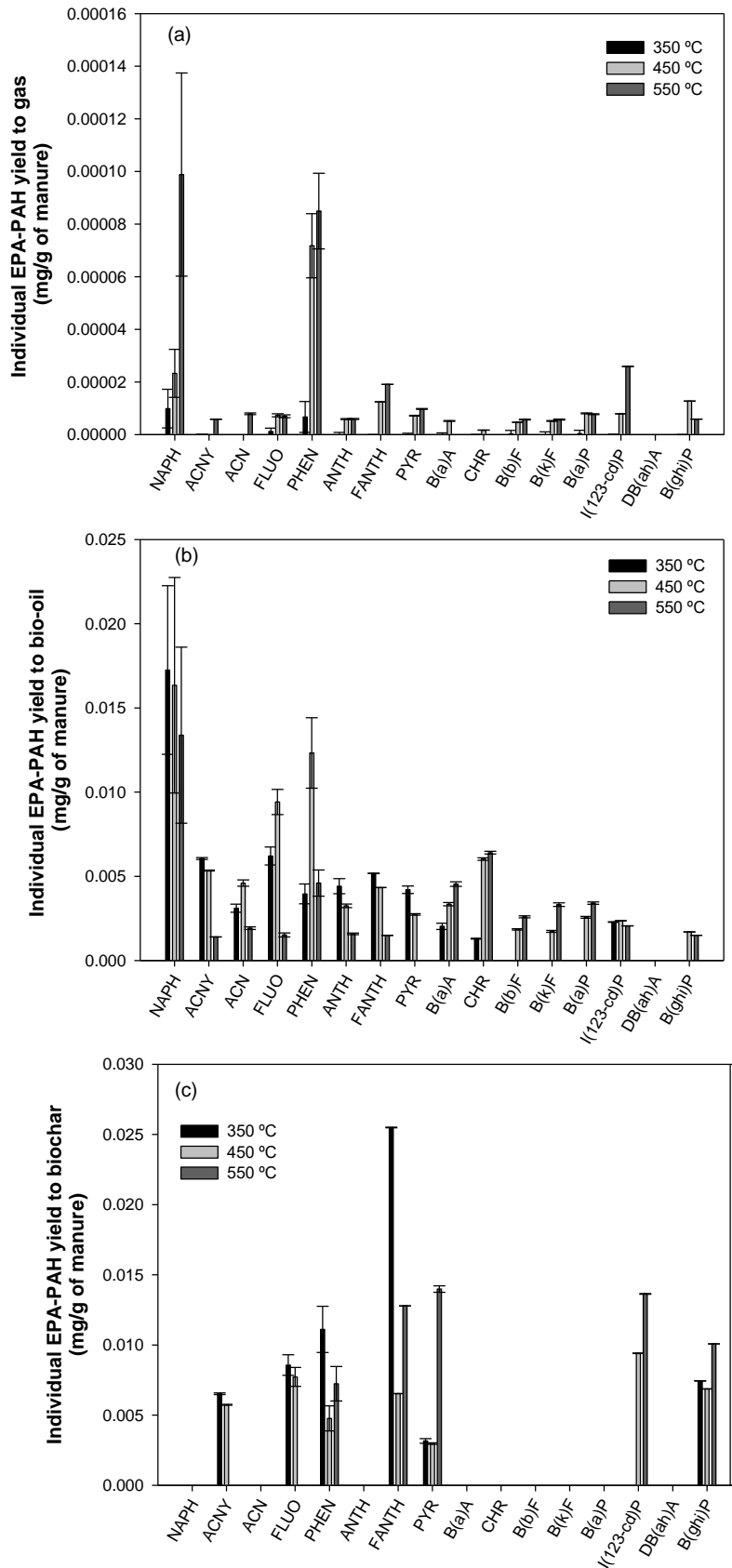
Fig. 5. Individual EPA-PAH yield in the three pyrolysis product fractions obtained from OS-PM: (a) liquid, (b) gas, (c) biochar (error bars show grouped standard deviation).

It can be seen that the liquid and the gas products contain almost all the 16 priority EPA-PAH (15 EPA-PAH in the liquid and 13 EPA-PAH in the gas), while the biochar only contains 7 of them. NAPH and PHEN were the EPA-PAH with the largest yields in both the liquid and the gas products. When comparing the distribution of the EPA-PAH in the liquid and the gas, it can be observed that the species with higher molecular weight were detected in the gas in lower proportions than in the liquid. This fact can be related to their higher boiling points, which would facilitate their condensation and collection in the liquid product. The solid product does not contain many of the low molecular weight EPA-PAH species, i.e. NAPH and ACNY, nor many of the high molecular weight ones, i.e. B[a]A, CHR, B[b]F, B[k]F and B[a]P. The lack of these compounds in the char could be caused either by their complete release from the solid particles or by their formation in gas phase reactions.

3.3 Biochar study

This section analyzes the EPA-PAH and B[a]P equivalent concentrations present in the feedstocks and in the biochars generated during the pyrolysis of the two different manures (OS-PM and CD-CM) at the three different temperatures (see Table 4).

Table 4. EPA-PAH and B[a]P equivalent concentrations in feedstocks and their biochars obtained at 350, 450 and 550 ºC.

	OS-PM-0	OS-PM-350	OS-PM-450	OS-PM-550	CD-CM-0	CD-CM-350	CD-CM-450	CD-CM-550
NAPH		0.0	0.0	0.0	0.105	0.396	0.110	0.041
ACNY		13.3	13.3	0.0	0.022	0.093	0.017	0.019
ACN		0.0	0.0	0.0	0.006	0.015	0.000	0.000
FLUO		17.5	17.9	0.0	0.012	0.062	0.004	0.002
PHEN	75	22.7	11.0	16.7	0.132	0.117	0.046	0.063
ANTH		0.0	0.0	0.0	0.014	0.019	0.005	0.006
FANTH	25	52.0	15.1	29.6	0.064	0.052	0.025	0.039
PYR	15	6.4	6.9	32.4	0.166	0.121	0.045	0.085
B[a]A		0.0	0.0	0.0	0.043	0.011	0.004	0.004
CHR		0.0	0.0	0.0	0.047	0.024	0.006	0.007
B[b]F		0.0	0.0	0.0	0.045	0.012	0.005	0.005
B[k]F		0.0	0.0	0.0	0.011	0.004	0.002	0.001
B[a]P		0.0	0.0	0.0	0.068	0.030	0.010	0.009
I[123-cd]P		0.0	21.8	31.6	0.025	0.066	0.007	0.004
DB[ah]A		0.0	0.0	0.0	0.011	0.052	0.000	0.000
B[ghi]P		15.2	15.9	23.3	0.078	0.131	0.035	0.016
Σ 16 EPA-PAH (mg·kg^{-1} of solid)	115	127.1	102.0	133.6	0.848	1.204	0.322	0.301

Σ B[a]P eq (mg·kg^{-1} of solid)	0.115	0.264	2.403	3.472	0.0933	0.0939	0.0125	0.0109

The pyrolysis treatment does not have a noticeable effect on the Σ16 EPA-PAH concentrations in the solids, obtaining biochars with concentrations close to those of their corresponding feedstock, although with small variations. These results are in agreement with those of Qiu et al. [21], who determined slightly higher or lower EPA-PAH concentrations in the biochar samples than in the feedstocks. Independently of these lesser differences, under the pyrolysis operating conditions used in this work, it can be said that the Σ16 EPA-PAH levels in the feedstock play a significant role in the levels found in their biochars.

The biochars obtained at 350 ℃ had slightly higher concentrations of Σ16 EPA-PAH than the feedstocks, especially for CD-CM. This suggests that most of the PAHs originally present in the manure remain in the solid and do not devolatilize at this temperature, but their concentration increases because they become more concentrated as other components of raw material release the solid matrix and the amount of solid matrix decreases. The boiling points shown in Fig. 1 indicate that at 450 and 550 ℃ most of the EPA-PAH compounds would have been devolatilized from the solid matrix ending up in the other two pyrolysis products. The Σ16 EPA-PAH concentrations in the biochars obtained at 450 ℃ from both feedstocks are lower than those found in the raw materials, meaning that their devolatilization from the solid matrix takes precedence over the reduction in the biochar yield (see Tables 2 and 4). In the case of CD-CM-450, the concentration of each of the 16 EPA-PAH decreases significantly in comparison with the biochar obtained at 350 ℃ (CD-CM-350). At 550 ℃, an increase (OS-PM-550) or a decrease (CD-PM-550) of the original EPA-PAH concentration in the feedstocks has been observed, depending on the feedstock used. The effect of the temperature on the degree of volatilization of the PAHs from the biochars, on their speciation (boiling points) and on the yields of biochar obtained at the different pyrolysis temperatures would explain the concentrations obtained at the three temperatures studied (see Table 4). Zielińska and Oleszczuk [17] obtained PAH concentrations in the biochar samples one order of magnitude lower than those in the feedstock (sewage sludge). These low PAH concentrations in the biochar could be explained by the high flow of nitrogen used in the fixed bed (630 cm^3·min^{-1}) by these authors, as opposed to 25 cm^3·min^{-1} used in

this work, which would favor the volatilization of the PAHs from the solid matrix during the pyrolysis reaction. In this regard, Buss et al. [9] observed that working with a high carrier gas flow, pyrolysis treatment could reduce the Σ16 EPA-PAH concentration of the biochar in comparison with biochars produced with lower flow-rates. Therefore, enhancing PAH volatilization from the solid matrix, e.g. using a higher flow-rate of carrier gas, would help to reduce the concentration of these contaminants in biochars.

As regards the PAH speciation, the biochars obtained from OS-PM contained the three PAHs originally present in the feedstock and two, three or four more species depending on the temperature used. In the case of the other feedstock (CD-CM-0), which already contained the 16 EPA-PAH, its biochars contained at least 14 of the 16 EPA-PAH. These results highlight the significant similarity between the PAH speciation of the feedstocks and those of the biochars obtained under the operational conditions studied. This relation suggests that the EPA-PAH compounds appearing after pyrolysis at low temperatures (<550 ºC) would come from the transformation of the PAH that the manure samples contained, as previously mentioned in connection with the EPA-PAH distribution study (see section 3.2). The increase in temperature results in a higher concentration of heavier PAH in the OS-PM biochars, although this effect is not appreciated for the biochars obtained from the CD-CM feedstock.

It is interesting to compare the Σ16 EPA-PAH concentrations in the biochar samples with the limits recommended by the IBI [5] and by the EBC [6]. All the biochars prepared under all of the operating conditions and with both feedstocks comply with the recommendation of IBI for Australia (300 mg·kg^{-1}), but only those generated from CD-CM are below the thresholds given by the IBI for Europe (6 mg·kg^{-1}) and by the EBC (12 mg·kg^{-1} for basic grade biochar and 4 mg·kg^{-1} for premium grade biochar). Therefore, in order to comply with the limits established by both the IBI and the EBC, the initial EPA-PAH concentration in the feedstock is a key factor.

Table 4 shows the B[a]P-eq concentration of the feedstocks and their biochars produced at the different temperatures. It can be seen that B[a]P-eq increases with the temperature for the OS-PM biochars, but decreases for the CD-CM. The low EPA-PAH concentration in the CD-CM biochars explains why the B[a]P-eq concentration was very low, considerably lower than the values obtained for the OS-PM biochars.

Even though the Σ16 EPA-PAH concentration in the biochars generated from OS-PM is similar to that present in the raw material, the different speciation of the EPA-PAH s leads to its significantly greater toxicity. This fact is related with the presence of high molecular weight EPA-PAH, such as I[123-cd]P and B[ghi]P. In the case of the biochar obtained from CD-CM, the slight decrease in the Σ16 EPA-PAH concentration in CD-CM-450 and CD-CM-550 causes significantly lower B[a]P-eq concentrations than in CD-CM-0 and CD-CM-350. With respect to B[a]P-eq, only the IBI, not the EBC, has a recommendation limit of 3 mg·kg^{-1} [5], and all the biochars, except OS-PM-550, fulfill this specification.

4. Conclusions

A qualitative and quantitative experimental study has been performed on the evolution of EPA-PAH compounds during the pyrolysis of two different manure samples, an outdoor-stored pig manure (OS-PM) and a co-digested cow manure (CD-CM), at different temperatures (350, 450 and 550 ºC), paying special attention to the occurrence of these compounds in the biochar.

The EPA-PAH mass balance closure results point to the absence of any significant net formation/disappearance of EPA-PAH compounds during low temperature pyrolysis (<550 ºC), although the EPA-PAH originally present in the feedstock are partially transformed into other EPA-PAH species. A systematic study with the macro components of the manure and model EPA-PAH compounds needs to be undertaken in order to explore the chemical mechanism governing this transformation. Under the operational conditions studied, EPA-PAH compounds are mostly found in the liquid and solid pyrolysis products, with negligible yields of these compounds in the pyrolysis gas. The distribution of the EPA-PAH between the three pyrolysis products is affected by the temperature. The lowest yield of EPA-PAH to the solid product and the highest to the liquid occurs at 450ºC. Heavier species of EPA-PAH, such as I[123-cd]P, DB[ah]A, and B[ghi]P, are observed in the biochar samples obtained from OS-PM as the pyrolysis temperature increases. These species are not observed in the biochars obtained from CD-CM. These differences in the evolution of the EPA-PAH speciation with temperature lead to opposite trends for the B[a]P equivalent concentration in the biochars obtained from OS-PM and CD-CM as the temperature increases.

The results obtained highlight that, at the pyrolysis temperatures studied (<550 ℃), the EPA-PAH concentration in the biochar is mainly governed by the concentration of these compounds in the feedstock and by their devolatilization during the pyrolysis reaction. Therefore, to control the occurrence of EPA-PAH in the pyrolysis biochar, the EPA-PAH concentration in the feedstock must be kept low.

Funding

5. References

[1] S. Jeffery, F.G.A. Verheijen, M. van der Velde, A.C. Bastos, A quantitative review of the effects of biochar application to soils on crop productivity using meta-analysis, Agric. Eco. Environ. 144 (2011) 175-187. https://doi.org/10.1016/j.agee.2011.08.015.
[2] C.J. Atkinson, J.D. Fitzgerald, N.A. Hipps, Potential mechanisms for achieving agricultural benefits from biochar application to temperate soils: a review, Plant Soil 337 (2010) 1-18. https://doi.org/10.1007/s11104-010-0464-5.
[3] S.P. Sohi, E. Krull, E. Lopez-Capel, R. Bol, A review of biochar and its use and function in soil, in: D.L. Sparks (Ed.) Advances in Agronomy, Vol 1052010, pp. 47-82.
[4] J. Lehmann, S. Joseph, Biochar for environmental management: science, technology and implementation, Second Edition. ed., Routledge, New York, 2015.
[5] Standardized Product Definition and Product Testing Guidelines for Biochar That Is Used in Soil, International Biochar Initiative, 2015.
[6] E.B. Fundation, European Biochar Certificate - Guidelines for a Sustainable Production of Biochar. Version 6.5E of 30th August 2018, European Biochar Foundation (EBC)Arbaz, Switzerland., 2018.
[7] S. Schimmelpfennig, B. Glaser, One step forward toward characterization: Some important material properties to distinguish biochars, J. Environ. Qual. 41 (2012) 1001-1013. https://doi.org/10.2134/jeq2011.0146.
[8] I. Hilber, F. Blum, J. Leifeld, H.P. Schmidt, T.D. Bucheli, Quantitative determination of PAHs in biochar: A prerequisite to ensure its quality and safe application, J. Agric. Food. Chem. 60 (2012) 3042-3050. https://doi.org/10.1021/jf205278v.

[9] W. Buss, M.C. Graham, G. MacKinnon, O. Mašek, Strategies for producing biochars with minimum PAH contamination, J. Anal. Appl. Pyrol. 119 (2016) 24-30. https://doi.org/10.1016/j.jaap.2016.04.001.

[10] S.E. Hale, J. Lehmann, D. Rutherford, A.R. Zimmerman, R.T. Bachmann, V. Shitumbanuma, A. O'Toole, K.L. Sundqvist, H.P.H. Arp, G. Cornelissen, Quantifying the total and bioavailable polycyclic aromatic hydrocarbons and dioxins in biochars, Environ. Sci. Technol. 46 (2012) 2830-2838. https://doi.org/10.1021/es203984k.

[11] S. Kloss, F. Zehetner, A. Dellantonio, R. Hamid, F. Ottner, V. Liedtke, M. Schwanninger, M.H. Gerzabek, G. Soja, Characterization of slow pyrolysis biochars: Effects of feedstocks and pyrolysis temperature on biochar properties, J. Environ. Qual. 41 (2012) 990-1000. https://doi.org/10.2134/jeq2011.0070.

[12] A. Freddo, C. Cai, B.J. Reid, Environmental contextualisation of potential toxic elements and polycyclic aromatic hydrocarbons in biochar, Environ. Pollut. 171 (2012) 18-24. https://doi.org/https://doi.org/10.1016/j.envpol.2012.07.009.

[13] J.M. De la Rosa, Á.M. Sánchez-Martín, P. Campos, A.Z. Miller, Effect of pyrolysis conditions on the total contents of polycyclic aromatic hydrocarbons in biochars produced from organic residues: Assessment of their hazard potential, Sci. Total Environ. 667 (2019) 578-585. https://doi.org/10.1016/j.scitotenv.2019.02.421.

[14] Z. Ma, Y. Yang, Y. Wu, J. Xu, H. Peng, X. Liu, W. Zhang, S. Wang, In-depth comparison of the physicochemical characteristics of bio-char derived from biomass pseudo components: Hemicellulose, cellulose, and lignin, Journal of Analytical and Applied Pyrolysis 140 (2019) 195-204. https://doi.org/https://doi.org/10.1016/j.jaap.2019.03.015.

[15] Z. Ma, Y. Yang, Q. Ma, H. Zhou, X. Luo, X. Liu, S. Wang, Evolution of the chemical composition, functional group, pore structure and crystallographic structure of bio-char from palm kernel shell pyrolysis under different temperatures, Journal of Analytical and Applied Pyrolysis 127 (2017) 350-359. https://doi.org/https://doi.org/10.1016/j.jaap.2017.07.015.

[16] M. Keiluweit, M. Kleber, M.A. Sparrow, B.R.T. Simoneit, F.G. Prahl, Solvent-extractable polycyclic aromatic hydrocarbons in biochar: Influence of pyrolysis temperature and feedstock, Environ. Sci. Technol. 46 (2012) 9333-9341. https://doi.org/10.1021/es302125k.

[17] A. Zielińska, P. Oleszczuk, The conversion of sewage sludge into biochar reduces polycyclic aromatic hydrocarbon content and ecotoxicity but increases trace metal content, Biomass Bioenergy 75 (2015) 235-244. https://doi.org/https://doi.org/10.1016/j.biombioe.2015.02.019.

[18] R.K. Sharma, M.R. Hajaligol, Effect of pyrolysis conditions on the formation of polycyclic aromatic hydrocarbons (PAHs) from polyphenolic compounds, J. Anal. Appl. Pyrol. 66 (2003) 123-144. https://doi.org/https://doi.org/10.1016/S0165-2370(02)00109-2.

[19] R.K. Sharma, J.B. Wooten, V.L. Baliga, X. Lin, W. Geoffrey Chan, M.R. Hajaligol, Characterization of chars from pyrolysis of lignin, Fuel 83 (2004) 1469-1482. https://doi.org/https://doi.org/10.1016/j.fuel.2003.11.015.

[20] H. Zhou, C. Wu, A. Meng, Y. Zhang, P.T. Williams, Effect of interactions of biomass constituents on polycyclic aromatic hydrocarbons (PAH) formation during fast pyrolysis, J. Anal. Appl. Pyrol. 110 (2014) 264-269. https://doi.org/https://doi.org/10.1016/j.jaap.2014.09.007.

[21] M. Qiu, K. Sun, J. Jin, L. Han, H. Sun, Y. Zhao, X. Xia, F. Wu, B. Xing, Metal/metalloid elements and polycyclic aromatic hydrocarbon in various biochars: The effect of feedstock, temperature, minerals, and properties, Environ. Pollut. 206 (2015) 298-305. https://doi.org/https://doi.org/10.1016/j.envpol.2015.07.026.

[22] L. Fagernäs, E. Kuoppala, P. Simell, Polycyclic Aromatic Hydrocarbons in Birch Wood Slow Pyrolysis Products, Energy Fuels 26 (2012) 6960-6970. https://doi.org/10.1021/ef3010515.

[23] A. Mohseni-Bandpei, M. Majlesi, M. Rafiee, S. Nojavan, P. Nowrouz, H. Zolfagharpour, Polycyclic aromatic hydrocarbons (PAHs) formation during the fast pyrolysis of hazardous health-care waste, Chemosphere (2019) 277-288. https://doi.org/10.1016/j.chemosphere.2019.04.028.

[24] L. Rey-Salgueiro, M.S. Garcia-Falcon, E. Martinez-Carballo, C. Gonzalez-Barreiro, J. Simal-Gandara, The use of manures for detection and quantification of polycyclic aromatic hydrocarbons and 3-hydroxybenzo[a]pyrene in animal husbandry, Sci. Total Environ. 406 (2008) 279-286. https://doi.org/10.1016/j.scitotenv.2008.07.059.

[25] L. Zhao, Y.H. Dong, H. Wang, Residues of organochlorine pesticides and polycyclic aromatic hydrocarbons in farm-raised livestock feeds and manures in Jiangsu, China, Sci. Total Environ. 450-451 (2013) 348-355. https://doi.org/10.1016/j.scitotenv.2012.09.017.

[26] K. Suominen, M. Verta, S. Marttinen, Hazardous organic compounds in biogas plant end products-Soil burden and risk to food safety, Sci. Total Environ. 491-492 (2014) 192-199. https://doi.org/10.1016/j.scitotenv.2014.02.036.

[27] D.R. Lide, CRC Handbook of Chemistry and Physics, CRC Press LLC, Boca Raton, 2004.

[28] W.H. Organization, Internationally Peer Reviewed Chemical Safety Information, World Health Organization, 2019.

[29] Libro del Web de Química del NIST, SRD 69, NIST (National Institute of Standards and Technology), NIST, 2019.

[30] TOXNET, Toxicology Data Network, U.S. National Library of Medicine, 2019.

[31] F. Liu, Y. Xu, J. Liu, D. Liu, J. Li, G. Zhang, X. Li, S. Zou, S. Lai, Atmospheric deposition of polycyclic aromatic hydrocarbons (PAHs) to a coastal site of Hong Kong, South China, Atmos. Environ. 69 (2013) 265-272. https://doi.org/https://doi.org/10.1016/j.atmosenv.2012.12.024.

[32] C. Qu, S. Albanese, A. Lima, D. Hope, P. Pond, A. Fortelli, N. Romano, P. Cerino, A. Pizzolante, B. De Vivo, The occurrence of OCPs, PCBs, and PAHs in the soil, air, and bulk deposition of the Naples metropolitan area, southern Italy: Implications for sources and environmental processes, Environ. Intern. 124 (2019) 89-97. https://doi.org/10.1016/j.envint.2018.12.031.

[33] N.E. Sánchez, J. Salafranca, A. Callejas, Á. Millera, R. Bilbao, M.U. Alzueta, Quantification of polycyclic aromatic hydrocarbons (PAHs) found in gas and particle phases from pyrolytic processes using gas chromatography–mass spectrometry (GC–MS), Fuel 107 (2013) 246-253. https://doi.org/https://doi.org/10.1016/j.fuel.2013.01.065.

[34] F. Viteri, M. Abián, Á. Millera, R. Bilbao, M.U. Alzueta, Ethylene–SO_2 interaction under sooting conditions: PAH formation, Fuel 184 (2016) 966-972. https://doi.org/10.1016/j.fuel.2016.01.069.

[35] N.E. Sánchez, A. Callejas, Á. Millera, R. Bilbao, M.U. Alzueta, Formation of PAH and soot during acetylene pyrolysis at different gas residence times and reaction temperatures, Energy 43 (2012) 30-36. https://doi.org/https://doi.org/10.1016/j.energy.2011.12.009.

[36] N.E. Sánchez, A. Callejas, Á. Millera, R. Bilbao, M.U. Alzueta, Polycyclic aromatic hydrocarbon (PAH) and soot formation in the pyrolysis of acetylene and ethylene: Effect of the reaction temperature, Energy Fuels 26 (2012) 4823-4829. https://doi.org/10.1021/ef300749q.

[37] J.T. McClave, T.L. Sicich, Statistics 9th Edition, Prentice Hall, Upper Saddle River, NJ, 2003.

[38] Y. Jia, D. Stone, W. Wang, J. Schrlau, S. Tao, S.L.M. Simonich, Estimated reduction in cancer risk due to PAH exposures if source control measures during the 2008 Beijing olympics were sustained, Environ. Health Perspect. 119 (2011) 815-820. https://doi.org/10.1289/ehp.1003100.

[39] M. Atienza-Martínez, J. Ábrego, G. Gea, F. Marías, Pyrolysis of dairy cattle manure: evolution of char characteristics, J. Anal. Appl. Pyrol. 145 (2020). https://doi.org/10.1016/j.jaap.2019.104724.

[40] N. Ruiz-Gómez, V. Quispe, J. Ábrego, M. Atienza-Martínez, M.B. Murillo, G. Gea, Co-pyrolysis of sewage sludge and manure, Waste Manage. (Oxford) 59 (2017) 211-221. https://doi.org/10.1016/j.wasman.2016.11.013.

[41] T. Liu, Y. Guo, N. Peng, Q. Lang, Y. Xia, C. Gai, Q. Zheng, Z. Liu, Identification and quantification of polycyclic aromatic hydrocarbons generated during pyrolysis of sewage sludge: Effect of hydrothermal carbonization pretreatment, J. Anal. Appl. Pyrol. 130 (2018) 249-255. https://doi.org/10.1016/j.jaap.2018.01.021.

[42] I. Fonts, M. Azuara, L. Lázaro, G. Gea, M.B. Murillo, Gas chromatography study of sewage sludge pyrolysis liquids obtained at different operational conditions in a fluidized bed, Ind. Eng. Chem. Res. 48 (2009) 5907-5915. https://doi.org/10.1021/ie900421a.

[43] A. D'Anna, Particle incorporation and growth: experimental evidences and a modelling attempt., in: H. Bockhorn, A. D'Anna, A.F. Sarafim (Eds.) In Combustion Generated Fine Particles., Karlsruhe University Press, Karlsruhe, 2008.

[44] H. Richter, J.B. Howard, Formation of polycyclic aromatic hydrocarbons and their growth to soot-a review of chemical reaction pathways, Prog. Energy Combust. Sci. 26 (2000) 565-608. https://doi.org/10.1016/s0360-1285(00)00009-5.